

Amel Ben Slimane
Mohamed M. Chehimi
Marie-Josèphe Vaulay

Polypyrrole-coated poly(vinyl chloride) powder particles: surface chemical and morphological characterisation by means of X-ray photoelectron spectroscopy and scanning electron microscopy

Received: 6 February 2003
Accepted: 21 May 2003
Published online: 27 June 2003
© Springer-Verlag 2003

A. Ben Slimane
Laboratoire de Chimie des Matériaux,
Faculté des Sciences de Bizerte,
7021 Bizerte, Tunisia

M.M. Chehimi (✉) · M.-J. Vaulay
Interfaces, Traitements,
Organisation et Dynamique des Systèmes,
Université Paris 7—Denis Diderot,
associé au CNRS (UMR 7086),
1 rue Guy de la Brosse, 75005 Paris, France
E-mail: chehimi@paris7.jussieu.fr

Abstract Polypyrrole (PPy)-coated poly(vinyl chloride) (PVC) powder particles were prepared by the in situ chemical polymerisation of pyrrole in aqueous solutions in the presence of PVC powder particles. The PVC particles in suspension served as a hydrophobic substrate for the in situ polymerisation of pyrrole using iron chloride as the oxidising agent and sodium *p*-toluene sulfonate. In these conditions, tosylate-doped PPy (PPyTS) was obtained and chlorides were inserted as minor codoping species. In some cases, the pyrrole was polymerised after incubating the PVC particles with poly(*N*-vinyl pyrrolidone). Scanning electron microscope (SEM) micrographs showed that the PVC particles retained their initial, quasispherical shape after coating by PPy. At low magnification, the coated PVC particles appeared smooth, but at high magnification, they exhibited a decoration by elementary nanoparticles

of about 200-nm size due to PPy bulk powder grains. Elemental analysis indicated a mass loading of PPy in the range 1–58% w/w. Specific surface analysis by X-ray photoelectron spectroscopy (XPS) resulted in the spectra of the PPy-coated PVC particles resembling those of bulk powder PPyTS even for low PPy mass loading. The surface fraction of PPy repeat units was found to vary in the 55–91% range. This result is consistent with the SEM observation of the PPy nanoparticles at the surface of PVC powder grains. However, despite the important loading of PPy, the XPS estimation of the overlayer thickness is in favour of a patchy coating rather than continuous coatings of PPy.

Keywords Polypyrrole · Poly (vinyl chloride) · Coatings · Composites · X-ray photoelectron spectroscopy

Introduction

Extensive research has been done over the last 30 years concerning conducting polymers. Among these, polypyrrole (PPy), polyaniline and polythiophene have been studied most widely to date [1, 2, 3]. These polymers have various potential applications, such as composite materials [4, 5], biomedical tests [6, 7, 8] and corrosion control of metal [9, 10].

PPy, a heterocyclic polymer, is one of the most promising conducting polymer because under certain

circumstances it may have high electrical conductivity [11], good environmental stability [12] and is easily synthesized. However, some factors currently limiting the applications of PPy include its poor mechanical strength and thus low processability, on the one hand, and high costs, on the other hand.

Improvement of these material properties can be achieved, for example, by forming hybrid organic/inorganic PPy (nano)composites [13, 14, 15], PPy blends with some commercially available insulating polymers, such as poly(alkyl methacrylate)s [16], PPy colloidal

particles [17] and PPy-coated polymer latex particles [8, 18, 19, 20, 21, 22, 23] or polymer powder [24]. All these approaches are well documented and the results from several laboratories indicated improvement of processability and conductivity.

Of relevance to the present work, poly(vinyl chloride) (PVC) powder particles were suspended in aqueous solutions and served as substrates for the in situ polymerisation of chloride-doped PPy (PPyCl) [24]. The main objectives were to improve the processability of PPy and study the electrical properties in relation to surface morphology of the PPy-coated particles.

Interfacial phenomena in composite materials are of paramount importance and require surface specific techniques to characterise the thermodynamics and chemistry of the interacting species. Actually, the long-term performance depends critically on the level of interaction and thus on the adhesion between the matrix and the discontinuous phase. For example, in PPy composite materials, the conducting polymer would act as the dispersed phase and the flexible polymer as the continuous one (matrix).

Understanding adhesion bonding at composite interfaces relies, partly, on the chemical information obtained by materials and adhesion scientists using X-ray photoelectron spectroscopy (XPS) and other (related) techniques. The interfacial chemistry is indeed a key parameter in understanding adsorption, wetting and adhesion of polymers and other materials.

As far as we are concerned, we have long used XPS to characterise interfacial properties of conducting PPy powders [25, 26, 27, 28], latexes [8, 23, 29, 30, 31, 32] and composites [14]. In the case of PPy powders, XPS was effective in studying their capacity to adsorb homopolymers [25], polymer blends [28] and diblock copolymers [27]. The extent of adsorbed flexible polymer was mainly related to the nature and physicochemical properties of the casting organic solvent.

This work concerns the reverse situation, that is, the formation of PPy coatings onto a flexible polymer powder, namely PVC. In previous work, we have used XPS to characterise polystyrene latex particles coated with PPy [8, 29, 30], polyaniline [31] and poly(ethoxydiethoxy thiophene) [32] in order to determine the surface coverage of the underlying insulating polymer latex by the conducting polymer coating. For example, high-surface-area latex particles were found to be poorly coated with PPy, whereas low-surface-area particles were fairly well coated with thick PPy overlayers. However, this is not the only important criterion for thick and homogeneous coatings of PPy. Several studies from our group conclusively showed that the hydrophobic nature of the substrate is an essential key in obtaining good PPy adhesion, the conducting polymer acting either as a substrate [33] or as a coating [34].

The aim of this work is to study by means of XPS the surface chemistry of PPy-coated PVC powder particles prepared in water in relation to the surface morphology examined by scanning electron microscopy (SEM), on the one hand, and the bulk chemical composition, on the other hand. The composite materials were prepared using a published protocol [24] where PVC acted as an organic, hydrophobic substrate for the in situ polymerisation of pyrrole using the oxidizing agent ferric iron chloride (III) and sodium *p*-toluene sulfonate (NaTS) for the insertion of *p*-toluene sulfonate (or tosylate) as the major dopant, chlorides being coinserted as minor ones. The preparation of tosylate-doped PPy (PPyTS) in the presence of PVC powder was preferred to that of PPyCl because the former is known to be much more stable than the latter [35, 36].

Experimental

Materials

Pyrrole (Acros) was purified by passing it through a column of activated basic alumina (Acros) prior to polymerisation. $\text{FeCl}_3 \cdot 6\text{H}_2\text{O}$ (Aldrich) and NaTS (supplied by Acros) were employed without further purification. PVC (molecular weight 180,000, Acros) and poly(*N*-vinyl pyrrolidone) (PVP) (molecular weight 24,000, Roth) were used as received. Water was distilled twice prior to use.

Synthesis of bulk powder PPyTS

Pyrrole (0.5 ml, 7.2 mmol) was added via a syringe to 100 ml of a stirred aqueous solution containing $\text{FeCl}_3 \cdot 6\text{H}_2\text{O}$ (4.87 g, 18 mmol) and NaTS (3.5 g) at room temperature. The oxidant-to-pyrrole molar ratio was 2.5, close to the optimal value recommended by Armes [37]. The reaction solution was stirred for 24 h and the resulting black precipitate was vacuum-filtered and washed with copious amounts of deionised water until the washings were clear. The powder was then dried in a desiccator overnight before characterisation.

Synthesis of PPy-coated PVC powder particles

PPy-coated PVC powder particles were synthesized under the same conditions as previously mentioned but in the presence of PVC particles. In two other cases, PVP was added to the reaction media. The proportions of the chemicals used for the preparation of the composites are summarised in Table 1. The composites are abbreviated by PPy-PVC-*x* and PPy-PVC-*x*-PVP, where *x* stands for the initial PVC-to-pyrrole ratio in grams per millilitre.

All the PPy-PVC-*x* were prepared as mentioned for PPyTS except that PVC particles were suspended in the oxidant solution prior to the addition of pyrrole.

In the case of the PVP-containing composites 1 and 2, the preparation procedure differed in the order of introducing PVP:

1. Composite 1: PVP was first dissolved in 100 ml water before introduction of $\text{FeCl}_3 \cdot 6\text{H}_2\text{O}$ and NaTS. Then PVC particles were suspended in the solution prior to introduction of pyrrole at once.

Table 1 Synthesis conditions of polypyrrole (PPy)-coated poly(vinyl chloride) (PVC) composites. Poly(*N*-vinyl pyrrolidone) is indicated by PVP

Pyrrole volume (ml)	PVC mass (g)	PVP mass (g)	Abbreviation ^b
0.5	1.5		PPy-PVC-3
0.5	2		PPy-PVC-4
0.5	12.5		PPy-PVC-25
0.25 ^a	12.5		PPy-PVC-50
0.5	12.5	1.25	PPy-PVC-25-PVP (1)
0.5	12.5	1.25	PPy-PVC-25-PVP (2)

^aThe initial volume of 0.25 ml pyrrole was used to avoid a massive absolute mass of PVC dispersed in a limited volume of aqueous solution. For 0.25 ml initial pyrrole volume, we used twice the lower initial concentrations of FeCl₃·6H₂O (2.44 g) and sodium *p*-toluene sulfonate (1.75 g)

^bThe number following PVC indicates the initial PVC-to-pyrrole ratio in grams per millilitre. Composites 1 and 2 correspond to two different procedures for preparing the composites using PVP (see text)

- Composite 2: PVP was first dissolved in water, then PVC particles were suspended. This step was meant to permit to the water-soluble PVP to adsorb onto the PVC particles prior to the insertion of the oxidant, NaTS and then pyrrole.

Elemental analysis

Bulk powder analyses were performed at the Service Central d'Analyse (Vernaison, France).

Scanning electron microscopy

SEM micrographs were obtained with a Cambridge 120 that was completely controlled using a computer workstation. The filament was zirconated tungsten and the accelerating voltage was set at 20 kV. All specimens were coated with gold prior to analysis in order to avoid or to limit static charging effects.

X-ray photoelectron spectroscopy

A Surface Science Instrument spectrometer equipped with a monochromatic Al K α X-ray source (1,486.6 eV) was used at a spot size of 1,000 μ m. The takeoff angle relative to the sample holder surface was 35°. The pressure in the analysis chamber was about 5 \times 10⁻⁹ mbar. The pass energy was set at 150 and 100 eV for the survey and the narrow scans, respectively. The step size was 1.12 eV for the survey spectra and 0.078 or 0.96 eV for the narrow scans. Charge compensation was achieved with a flood gun of 0–3-eV electrons and a nickel grid placed 1 mm above the powder specimen holder. In these conditions, only the powder under test could be analysed by XPS and absolutely not the nickel grid (see later). Data processing was achieved with Win-spec software, kindly supplied by the Laboratoire Interdisciplinaire de Spectroscopie d'Electrons (Namur, Belgium). The spectra were calibrated against the main N 1s peak from PPy centred at 399.7 eV [38]. The surface composition was determined using the manufacturer's sensitivity factors. The fractional concentration of a particular element, *A* (% *A*), was computed using

$$\%A = \frac{(I_A/s_A)}{\sum (I_n/s_n)} \times 100\%, \quad (1)$$

where *I_n* and *s_n* are the integrated peak areas and the sensitivity factors, respectively.

Results and discussion

All PPy-PVC-*x* composites were black as bulk powder PPyTS. However, the PPy-PVC-*x*-PVP composite powders were dark greyish indicating a lower mass loading of PPy.

Scanning electron microscopy

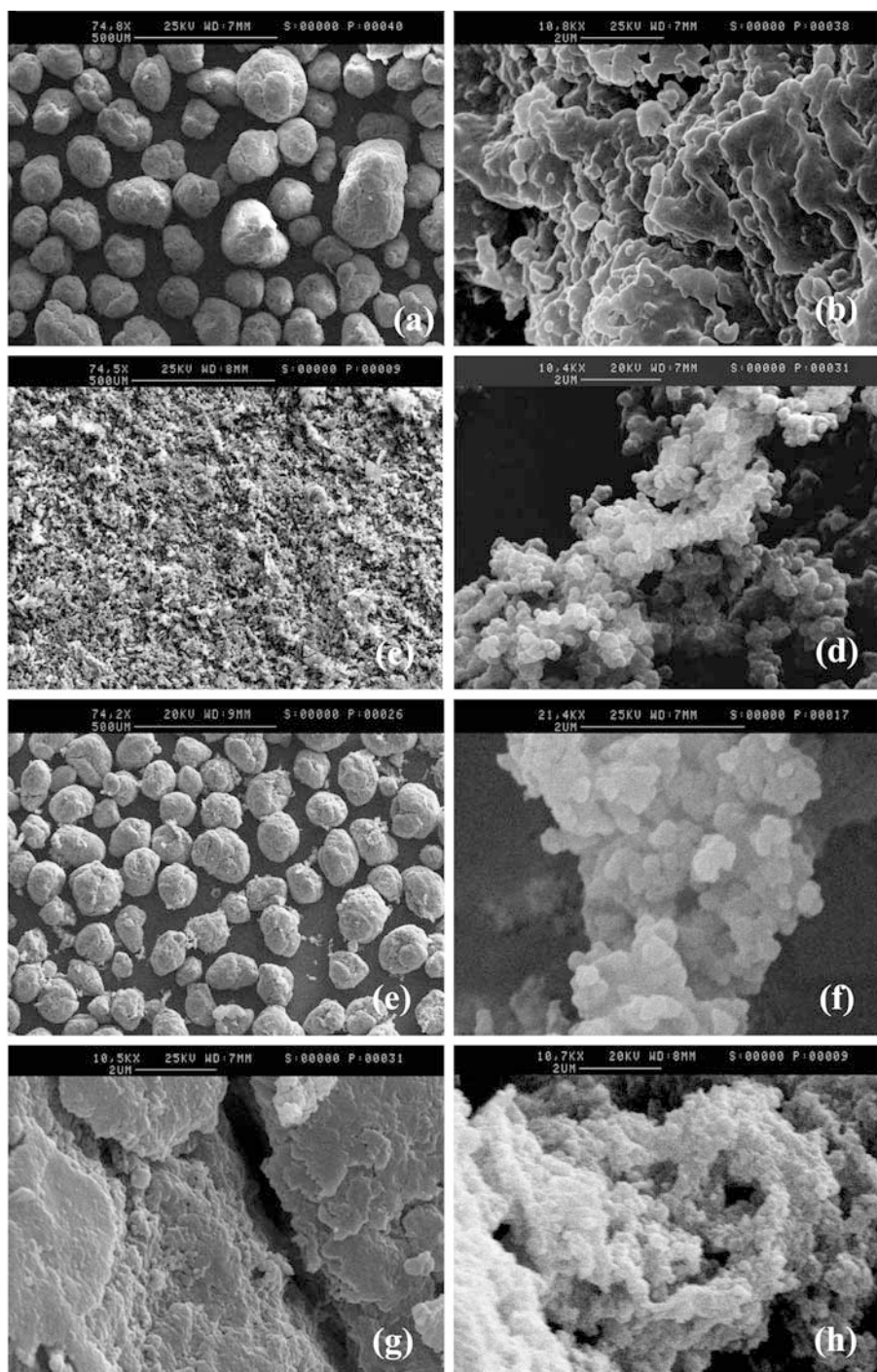
SEM micrographs of PVC, PPyTS, PPy-PVC-25 and PPy-PVC-25-PVP (1) and (2) are shown in Fig. 1. PVC exhibits polydisperse spherical or ovoid powder particles (Fig. 1a) and exhibits the morphology of molten wax (Fig. 1b) at higher magnification (x10,000). PPyTS looks like a spongy material (Fig. 1c) at low magnification (x75) and exhibits a nodular structure (Fig. 1d) with nanoparticles in the 200-nm size range at high magnification (x10,000). At low magnification, PPy-PVC-25 (Fig. 1e) appears spherical and smooth but at high magnification (x21,000), the powder particles exhibit a nodular aspect (Fig. 1f) similar to that of PPyTS. One can see at low magnification debris due to precipitating PPyTS, a situation similar to that encountered with PPy-coated silica gel particles [39]. It is interesting to note that for low initial PVC mass, the PPy-PVC-3 composite exhibits a structure as shown in Fig. 1c with some buried PVC grains, an indication of the high loading of PPy as precipitating powder in addition to surface coating.

PPy-PVC-25-PVP (1) (SEM image at low magnification similar to that in Fig. 1e) also exhibits debris but to a lesser extent. This is almost not at all the case of the PPy-PVC-25-PVP (2) composite, which has a structure similar to that shown for uncoated PVC (Fig. 1a). For high magnification, Fig. 1h shows the nodular structure of PPy ad-layers. Despite the dark colour of PPy-PVC-25-PVP (1), the surface morphology at high magnification (x10,000) is between the structures of PVC and PPyTS displayed in Fig. 1b and d, respectively. Therefore, the chronological order of introduction of PVP and other species has an important effect on the final morphology of PPy-PVC composites.

Elemental analysis

The elemental analysis of PPy-PVC-*x*, PPy-PVC-25-PVP and the reference PPyTS powder is reported in Table 2. In the case of PPyTS, chlorine is due to the coinserction of chlorides to dope PPy. The extent of chlorine is massive in the composites since it is essen-

Fig. 1 Scanning electron micrographs of **a** untreated poly(vinyl chloride) (*PVC*) powder at low magnification (x74.8), **b** *PVC* powder at high magnification (x10,800), **c** tosylate-doped polypyrrole (*PPyTS*) bulk powder at x74.5 magnification, **d** *PPyTS* at x10,400 magnification, **e** *PPy-PVC-25* at x74.2 magnification, **f** *PPy-PVC-25* at x21,400 magnification, **g** *PPy-PVC-25-PVP* (1) at x10,500 magnification, **h** *PPy-PVC-25-PVP* (2) at x10,700 magnification



tially due to the underlying *PVC*. The highest content of chlorine was obtained for the *PVP*-containing composites, again another result that is in line with the greyish colour of such composites.

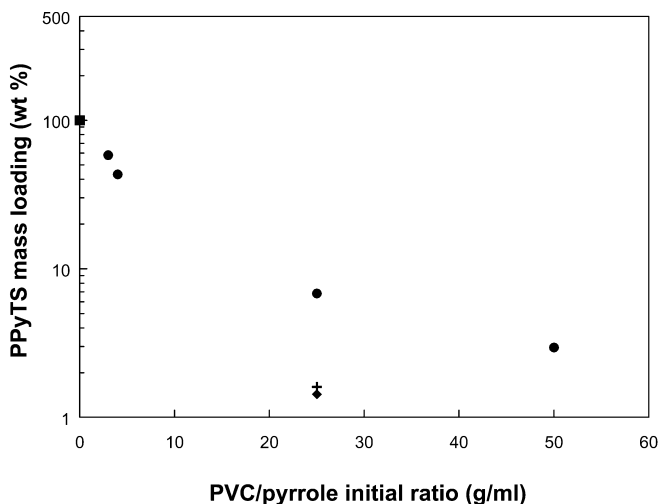
From the weight percent of nitrogen reported for the *PPyTS* and for *PPy-PVC-x*, the mass loading of *PPyTS* can be estimated:

$$(\%PPyTS)_{\text{composite}} = (\%N)_{\text{composite}} / (\%N)_{PPyTS} \quad (2)$$

The *PPyTS* mass loading is plotted in Fig. 2 versus the initial *PVC*/pyrrole ratio expressed in grams of *PVC* per volume of pyrrole monomer. Clearly, there is a monotonic decrease of *PPyTS* (weight percent) when the initial *PVC*

Table 2 Elemental analysis (wt%) of PPy-coated PVC powder particles. tosylate-doped PPy is represented by PPyTS

Abbreviation	C	N	Cl
PPyTS	54.67	11.87	3.14
PPy-PVC-3	43.99	6.91	24.91
PPy-PVC-4	42.23	5.13	36.0
PPy-PVC-25	38.29	0.81	49.99
PPy-PVC-50	39.06	0.35	46.16
PPy-PVC-25-PVP (1)	38.98	0.19	54.61
PPy-PVC-25-PVP (2)	38.35	0.17	54.26

**Fig. 2** PPy mass loading versus the initial PVC-to-pyrrole ratio for PPyTS (square), PPy-PVC composites (circles), PPy-PVC-PVP (1) (cross) and PPy-PVC-PVP (2) (diamond)

mass is increased. When the same composites are prepared using PVP, there is a distinctly lower PPyTS loading that is at best equal to 1.6 and 1.43% for PPy-PVC-25-PVP (1) and PPy-PVC-25-PVP (2), respectively, if of course PVP is neglected. However, since PVP is a component of the end composites, it contributes to the nitrogen weight percent; hence, a lower PPyTS mass loading than indicated in Fig. 2 results.

X-ray photoelectron spectroscopy

The survey scans of PPyTS, PPy-PVC-3 and PPy-PVC-50 are shown in Fig. 3. The main peaks are C 1s, N 1s and O 1s centred at 285, 400 and 531 eV, respectively. The minor peaks S 2p (168 eV) and Cl 2p (around 200 eV) are assigned to the tosylate dopants and to chloride and/or PVC, respectively. There is also evidence for the existence of iron at the surface of PPyTS and the PPy-PVC composites (Fe 2p_{3/2} at around 710 eV). The N 1s peak intensity substantially decreases with the initial mass of PVC, an indication that PPyTS is patchy

or not very thick (thickness less than 10 nm, the depth probed by XPS).

For PPyTS, Cl 2p is due to the insertion of the codopant chlorides and also FeCl₂ [29]. In the case of all the composites, Cl 2p is as (more) intense as (than) S 2p as shown in Fig. 3b and c.

The C 1s structures of PPyTS and PPy-PVC-50 are displayed in Fig. 4. The PPyTS C 1s peak tails and is fitted with six components due to aromatic (from tosylate dopant) and β -type carbons, the C-N atoms and three types of carbons due to surface oxidation and defects. The last component, centred at 291.6 eV, is due to a shake-up satellite associated with the conjugated structure of PPy and the aromatic character of the tosylate dopant. It is noteworthy that the C 1s peak-tailing is much hindered when PPyTS is coated on PVC particles owing to the strong contribution of the underlying PVC (Fig. 4b). In this case, the two components at the highest binding energy (289.6 and 291.5 eV) practically do not contribute to the overall structure. It is worth noting that the second component has an appreciable relative intensity owing to the contribution of CC/CH carbon type in PVC.

The narrow N 1s regions from PPyTS bulk powder and the PPy-PVC-25-PVP (1) composite are depicted in Fig. 5. The N 1s region from PPyTS has a typical shape that can be fitted with four components centred at 398.5, 399.7, 401.5 and 404.1 eV that are assigned to C=N defects, the N-H pyrrole bond and two types of positively charged nitrogens, respectively. In the case of the composite prepared with PVP, a similar shape is exhibited by the N 1s region, however with an obvious effect of the N 1s region from PVP that overlaps that of the PPy coating. This direct detection of PVP is in line with the lesser extent of the imine defects and the positively charged nitrogen atoms from PPy. Indeed, PVP contributes to the main component centred at 399.7 eV, very close to its reference value of 399.9 eV [40].

High-resolution Cl 2p regions for PPyTS and PPy-PVC-3 are depicted in Fig. 6. As shown Kang et al. [38], the Cl 2p from the PPy chloride dopants has a complex structure that can be fitted with three components. In our case, the Cl 2p structure displayed in Fig. 6a is fitted with only two components, centred at 197.3 and 199.8 eV, which we refer to as Cl_I and Cl_{II}. Note this doublet is not due to a spin-orbit splitting but to two distinct chlorine species, the first being chlorides. The Cl_{II} species could be due to a different type of interaction of chlorides with the PPy backbone [38]. This has actually been discussed at length elsewhere, and here we simply use the spectrum in Fig. 6a as a fingerprint of the PPy codopant when dealing with the Cl 2p features from the composites. In Fig. 6b, the Cl 2p region from PPy-PVC-3 exhibits a shoulder at low binding energy by contrast to PPy and this is due to the underlying PVC that has a peak component centred at 200.5 eV. In Fig. 6b, the two first minor peaks correspond to Cl_I and

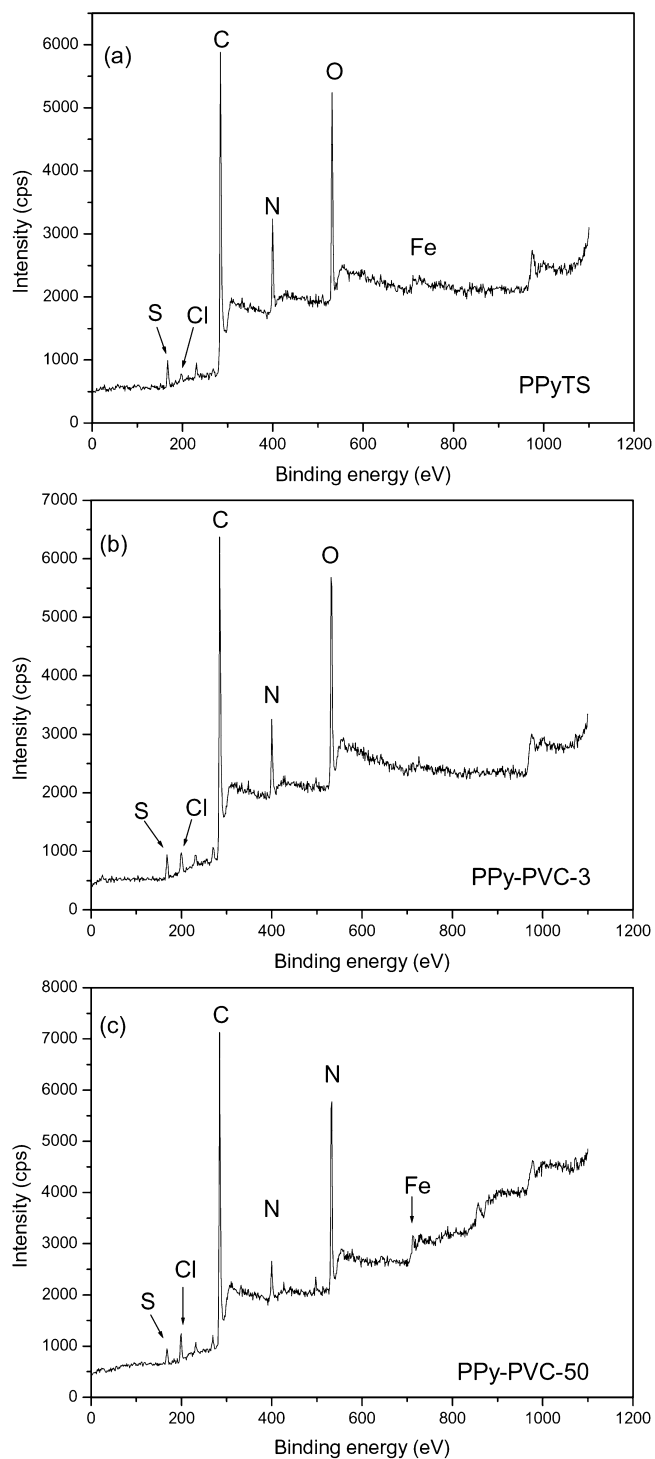


Fig. 3 X-ray photoelectron spectroscopy survey scans of **a** PPyTS bulk powder, **b** PPy-PVC-3, **c** PPy-PVC-50

Cl_{II} types from PPyTS. Here, it is assumed that the $\text{Cl}_I/\text{Cl}_{II}$ and $\text{Cl } 2p/\text{S } 2s$ intensity ratios remain the same by comparison to bulk powder PPyTS. The surface composition in atomic percent is reported in Table 3.

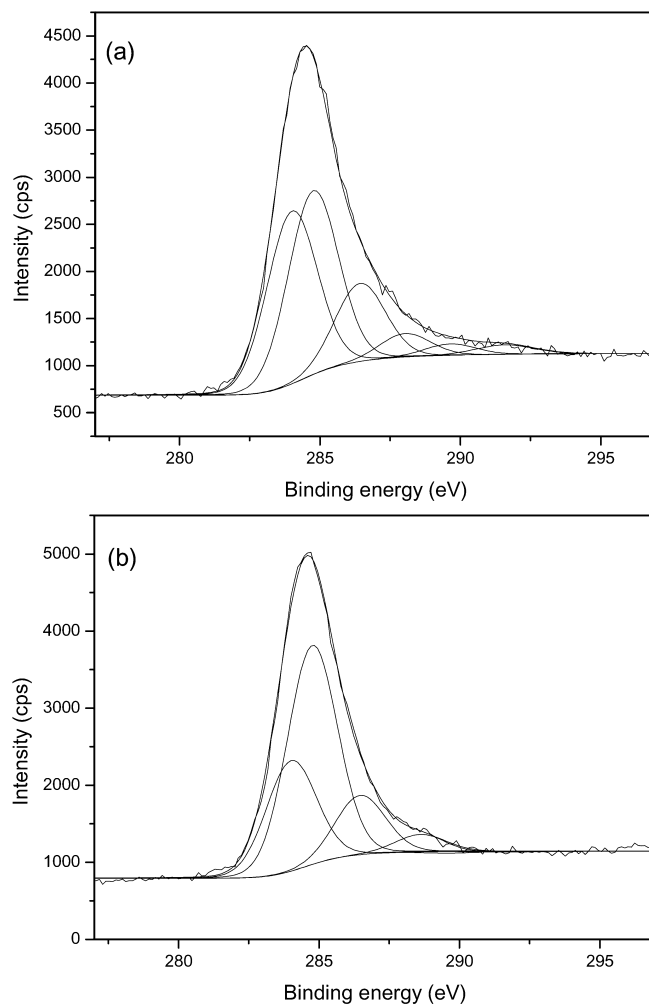


Fig. 4 High-resolution C 1s regions of **a** PPyTS bulk powder, **b** PPy-PVC-50

The doping level for PPyTS powder and composites was determined by

$$\text{Doping} = (S + \text{Cl}_{\text{PPy}}) / N (\%), \quad (3)$$

where S and N are the sulfur and nitrogen atomic percents. Since sulfur is the main component, the sulfur-to-nitrogen ratio is plotted in Fig. 7 versus the initial mass of PVC. The horizontal dashed line stands for the average value of the sulfur-to-nitrogen ratio for PPyTS and PPy-PVC composites. PPy appears very well doped regardless of whether it is prepared as a bulk powder or as a composite. It is to be noted that for the PVP-containing composites the sulfur-to-nitrogen ratios are significantly lower than those corresponding to PPyTS and the PPy-PVC- x series. This is simply due to the incorporation of PVP (contains one N atom per repeat unit) in the PPy-PVC-25-PVP composites.

Assuming that the chlorine-to nitrogen, r_{Cl} , and sulfur-to-nitrogen, r_{S} , atomic ratios determined for PPyTS

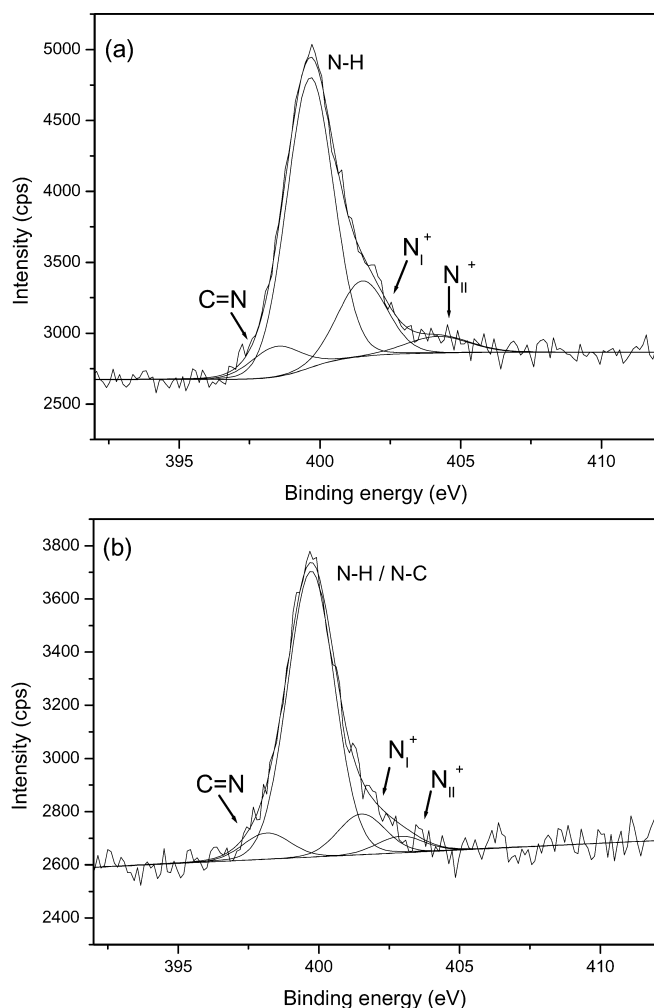


Fig. 5 High-resolution N 1s regions of **a** PPyTS bulk powder, **b** PPy-PVC-25-PVP(1)

bulk powder remain the same for the composite specimens, one can calculate the surface composition in molar percent of pyrrole, vinyl chloride and *N*-vinyl pyrrolidone repeat units. These are called %PPy, %PVC and %PVP, respectively. For PPy-PVC-*x* composites, the relative proportions of PPyTS and PVC are calculated as follows:

$$\%PPy = N_{PPy} / (N_{PPy} + Cl_{PVC}), \quad (4)$$

where N_{PPy} and Cl_{PVC} are the nitrogen content from PPy and the chlorine content from PVC, respectively. It follows that in practice

$$\%PPy = N_{PPy} / (N_{PPy} + Cl - r_{Cl}N_{PPy}) = N / (N + Cl - r_{Cl}N) \quad (5)$$

and

$$\%PVC = 100 - \%PPy, \quad (6)$$

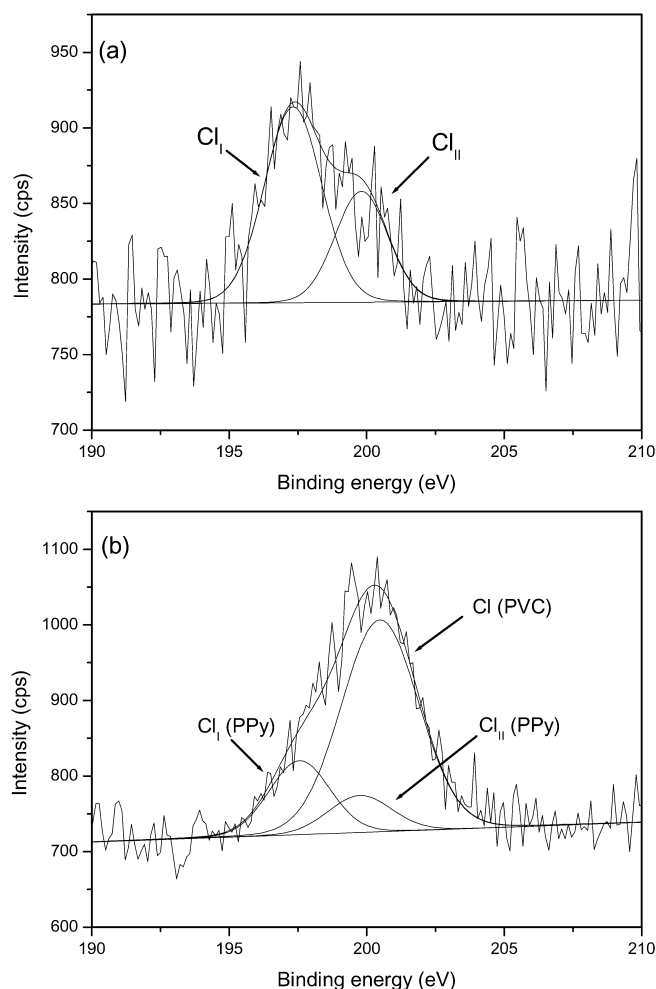


Fig. 6 High-resolution Cl 2p regions of **a** PPyTS bulk powder, **b** PPy-PVC-3

where N and Cl are the nitrogen and chloride atomic percents reported in Table 3 and r_{Cl} is as defined earlier. In Eq. (5), the contribution of the chloride dopants is subtracted from the total chlorine content in order to determine Cl_{PVC} .

For PP-PVC-25-PVP composites, both PVP and PPy contribute to the nitrogen content, on the one hand, and

Table 3 Surface composition (atom%) of PPy-coated PVC powder particles

Abbreviation	C	N	O	S	Cl	Fe
PPyTS	68.2	10.6	17.0	3.00	1.04	0.15
PPy-PVC-3	66.3	8.67	20.2	2.55	2.35	0
PPy-PVC-4	72.7	8.34	15.1	2.22	1.64	0
PPy-PVC-25	72.7	5.86	17.4	1.57	1.79	0.66
PPy-PVC-50	70.6	4.88	19.2	1.69	3.04	0.62
PPy-PVC-25-PVP (1)	75.3	5.54	15.1	1.17	2.14	0.69
PPy-PVC-25-PVP (2)	66.1	8.30	17.7	1.85	4.12	1.93

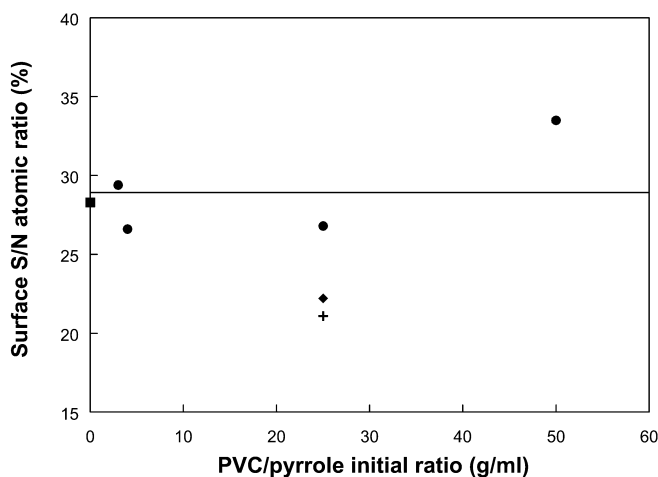


Fig. 7 Surface sulfur-to-nitrogen atomic ratio versus the initial PVC-to-pyrrole ratio for bulk powder PPy: PPyTS (square), PPy-PVC composites (circles), PPy-PVC-PVP (1) (cross), and PPy-PVC-PVP (2) (diamond)

PPyTS and PVC contribute to the chlorine content, on the other hand. Therefore, the nitrogen from PPyTS (N_{PPy}) can be estimated by

$$N_{\text{PPy}} = S/r_S. \quad (7)$$

It follows that the contribution of PVP to nitrogen (N_{PVP}) can be calculated by

$$N_{\text{PVP}} = N - (S/r_S), \quad (8)$$

where N is the total nitrogen atomic percent reported for the composites in Table 3. The relative proportion of PVC (%PVC) can be estimated by determining the contribution of PVC to the total chlorine content:

$$\text{CI}_{\text{PVC}} = \text{CI} - \text{CI}_{\text{PPy}} = \text{CI} - r_{\text{Cl}} N_{\text{PPy}}. \quad (9)$$

It follows that

$$\text{CI}_{\text{PVC}} = \text{CI} - r_{\text{Cl}} (S/r_S). \quad (10)$$

The relative proportions of PPyTS, PVC and PVP can then be calculated as follows:

$$\% \text{PPy} = N_{\text{PPy}} \times 100\% / (N_{\text{PPy}} + N_{\text{PVP}} + \text{CI}_{\text{PVC}}), \quad (11a)$$

$$\% \text{PVP} = N_{\text{PVP}} \times 100\% / (N_{\text{PPy}} + N_{\text{PVP}} + \text{CI}_{\text{PVC}}), \quad (11b)$$

$$\% \text{PVC} = \text{CI}_{\text{PVC}} \times 100\% / (N_{\text{PPy}} + N_{\text{PVP}} + \text{CI}_{\text{PVC}}). \quad (11c)$$

The XPS data of the N 1s peak from PPyTS bulk powder and the composites permit the thickness of the conducting polymer at the surface of PVC powder particles to be estimated. For the PPyTS overlayer, the N 1s peak intensity in the composites, I , can be expressed by

$$I = I_0 \times [1 - \exp(-d/\lambda \sin \theta)], \quad (12)$$

where I_0 is the bulk powder N 1s intensity, d is the thickness of PPyTS overlayers, λ is the mean free path of the N 1s core electrons in the PPyTS overlayer, and θ is the take off angle relative to the surface [41]. For spherical substrates, the average value for $\sin \theta$ is 0.5 [42]. The expression for λ is given by [41]

$$\lambda \approx 0.11 E_K^{0.5} \left(\text{mg/m}^2 \right), \quad (13)$$

where E_K is the kinetic energy of the ejected core-hole electron. Dividing λ in milligrams per metre squared by the density of the overlayer (approximately 1.5 for PPy) yields a value of λ in nanometres. For N 1s electrons ejected from PPyTS and travelling through their own material, i.e. the conducting overlayer, the mean free path is $\lambda_{\text{N 1s}} = 2.42$ nm. With this value in hand and all values of $I(\text{N 1s})$ obtained with the composites and $I_0(\text{N 1s})$ obtained with bulk powder PPyTS, the average thickness values of PPy overlayers can be determined, with the assumption they are uniform. The average thickness of the PPyTS overlayers and the surface fractions of PPyTS, PVC and PVP (determined using Eq. 11a, 11b, 11c) for all the composite materials investigated are reported in Table 4.

The surface concentration of PPy is very important especially for an initial PVC/pyrrole ratio of 3 and 4 g/ml. For a higher value of this ratio, the PPy surface fraction remains quite important. The surface fraction of PPy is plotted against its bulk fraction determined for the PPy-PVC composites and the reference PPyTS powder in Fig. 8. Clearly, a very low bulk molar fraction (1.9%) of pyrrole repeat units (corresponding to a PPy mass loading of around 3 wt%) yields a high surface fraction of 66.4% in pyrrole repeat units. These results are consistent with the electrical conductivity measurements reported by Ouyang and Chan [24] as a function of the PPy mass loading. The percolation threshold value found by these authors was 0.3 wt% and the corresponding composite was 10 orders of magnitude more conductive than PVC. The PPy overlayer thicknesses are lower than 3 nm (6 nm at best if $\sin \theta = 1$). This value is much lower than the 200 nm size of the PPy nanopar-

Table 4 Relative proportions of polymer repeat units and PPyTS overlayer thickness at the surface of PPy-coated PVC powders

Materials	PPy	PVC	PVP	d (nm)
PPyTS	100			
PPy-PVC-3	85.3	14.7		2.9
PPy-PVC-4	91.1	8.9		1.2
PPy-PVC-25	82.9	17.1		0.85
PPy-PVC-50	66.4	33.6		0.74
PPy-PVC-25-PVP (1)	56.6	23.8	19.6	0.48
PPy-PVC-25-PVP (2)	55.3	29.5	15.2	0.66

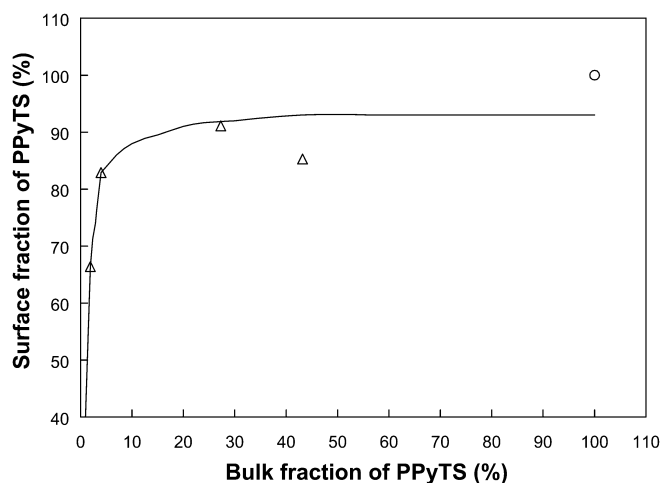


Fig. 8 Surface fraction of PPy repeat units versus the bulk fraction of PPy in molar percent of pyrrole repeat units: PPyTS (circle), PPy-PVC composites (diamonds)

ticles observed by SEM at the surface of PVC. The results suggest therefore a patchy deposition of PPy despite the deep black colour of the composites.

Conclusion

PPyTS was coated on PVC powder particles by the in situ chemical polymerisation of pyrrole in water, using FeCl_3 as the oxidising agent in the presence of NaTS. Massive loadings of PPy were obtained confirming published literature data [24], resulting in XPS spectra, the structures of which are very similar to those of bulk powder PPy. SEM micrographs exhibited the nodular

structure of PPy at the surface of PVC with elementary PPyTS nanoparticles having a diameter of about 200 nm.

The surface morphology was monitored as a function of the initial PVC-to-pyrrole ratio in grams per millilitre. High values of this ratio permit thin overlayers of PPy to be obtained. At a low initial PVC-to-pyrrole ratio, the composite materials consisted of PPy-coated PVC and precipitating PPyTS.

Another way of preparing such composites was presented: pre-coating the PVC particles with PVP. This method, leads to very low PPy mass loadings but that are more confined to the PVC essentially as a thin overlayer and with very little amount of debris.

A thorough XPS analysis of the composites indicated a strong and quasiconstant level of doping of PPy and a very PPy-rich surface of the composites for all PPy mass loadings. Plots of the PPy surface fraction versus the bulk fraction of pyrrole repeat units indicate a threshold of less than 3 wt%, a result that has to be connected with conductivity measurements reported in the literature [24]. Moreover, we used PPyTS, a much more hydrophobic PPy than PPyCl [33]; therefore, favourable hydrophobic interactions at the PPyTS-PVC interface are likely to occur and to govern at least partly the encapsulation of PVC powder particles. However, investigation of the PPyTS N 1s peak attenuation permitted an average thickness of 3–6 nm to be estimated; this is much lower than the size of the PPy nanoparticles, an indication of patchy overlayers.

Acknowledgements A.B. is indebted to the University of Paris VII and the EGIDE institution for financial support through a professorship and research training scheme, respectively. All coauthors thank Pascal Bargiela for technical assistance with XPS measurements.

References

- Aldissi M (ed) (1993) *Intrinsically conducting polymers: an emerging technology*. Kluwer, Dordrecht
- Nalwa HS (ed) (1997) *Handbook of organic conducting molecules and polymers*, vol 2, Wiley, Chichester
- Skotheim TA, Elsenbaumer RL, Reynolds JR (eds) (1998) *Handbook of conducting polymers*, 2nd edn. Dekker, New York
- Rodriguez J, Grande H, Otero TF (1997) In: Nalwa HS (ed) *Handbook of organic conducting molecules and polymers*, vol 2, Wiley, Chichester, pp 415–468
- Gangopadhyay R, De A (2000) *Chem Mater* 12:608
- Miksa B, Slomkowski S (1995) *Colloid Polym Sci* 273:47
- Pope MR, Armes SP, Tarcha P (1996) *Bioconjugate Chem* 7:436
- Chehimi MM, Azioune A, Bousalem S, Ben Slimane A, Yassar A In: Elaissari A (ed) *Colloid polymers: preparation and biomedical applications*. Dekker, New York (in press)
- Tallman DE, Pae Y, Bierwagen GP (2000) *Corrosion* 56:401
- Ferreira CA, Domenech SC, Lacaze PC (2001) *J Appl Electrochem* 31:49
- Kathirgamanathan P (1991) In: Fawcett AH (ed) *High value polymers*. Royal Society of Chemistry, Cambridge, pp 174–205
- Omastová M, Košina S, Pionteck J, Janke A, Pavlinec J (1996) *Synth Met* 81:49
- Maeda S, Armes SP (1993) *J Colloid Interface Sci* 159:257
- Perruchot C, Chehimi MM, Delamar M, Fievet F (1998) *Surf Interface Anal* 26:689
- Cho G, Glatzhofer DT, Fung BM, Yuan W-L, O'Rear EA (2000) *Langmuir* 16:4424
- Ruckenstein E, Wang S (1993) *Polymer* 34:4655
- Armes SP, Vincent B (1987) *J Chem Soc Chem Commun* 288
- Yassar A, Roncali J, Garnier F (1987) *Polym Commun* 28:103

19. Wiersma AE, Steeg LMA, Jongeling TJM (1995) *Synth Met* 71:2269
20. Khan MA, Armes SP (2000) *Adv Mater* 12:671
21. Omastová M, Pavlinec J, Pionteck J, Simon F, Kosina S (1998) *Polymer* 39:6559
22. Omastová M, Simon F (2000) *J Mater Sci* 35:1743
23. Bousalem S, Yassar A, Basinska T, Miksa B, Slomkowski S, Azioune A, Chehimi MM (2003) *Polym Adv Technol* (in press)
24. Ouyang M, Chan CM (1998) *Polymer* 39:1857
25. Abel M-L, Chehimi MM (1994) *Synth Met* 66:225
26. Chehimi MM, Abel M-L, Saoudi B, Delamar M, Jammul N, Watts JF, Zhdan PA (1996) *Polimery* 41:75
27. Chehimi MM, Abel M-L, Fricker F, Delamar M, Jada A, Brown AM, Watts JF (1998) *J Chim Phys* 95:1282
28. Abel M-L, Chehimi MM, Fricker F, Delamar M, Brown AM, Watts JF (2002) *J Chromatogr A* 969:273
29. Perruchot C, Chehimi MM, Delamar M, Lascelles SF, Armes SP (1996) *Langmuir* 12:3245
30. Cairns DB, Armes SP, Chehimi MM, Perruchot C, Delamar M (1999) *Langmuir* 15:8059
31. Barthet C, Armes SP, Chehimi MM, Bilem C, Omastova M (1998) *Langmuir* 14:5032
32. Khan MA, Armes SP, Perruchot C, Ouamara H, Chehimi MM, Greaves SJ, Watts JF (2000) *Langmuir* 16:4171
33. Azioune A, Chehimi MM, Miksa B, Basinska T, Slomkowski S (2002) *Langmuir* 18:1150
34. Perruchot C, Chehimi MM, Delamar M, Cabet-Deliry E, Miksa B, Slomkowski S, Khan MA, Armes SP (2000) *Colloid Polym Sci* 278:1139
35. Armes SP, Aldissi M (1990) *Polymer* 31:569
36. (a) Chehimi MM, Abel M-L, Sahraoui Z, Fraoua K, Lascelles SF, Armes SP (1997) *Int J Adhes Adhes* 17:1; (b) Chehimi MM, Abdeljalil E (2002) Paper presented at Modification, degradation and stabilisation of polymers (MODEST 2002) conference, Budapest, Hungary; (c) Chehimi MM, Abdeljalil E *Polym Degrad Stab* (submitted)
37. Armes SP (1987) *Synth Met* 20:365
38. Kang ET, Neoh KG, Tan KL (1993) *Adv Polym Sci* 106:135
39. Perruchot C (2000) PhD thesis. University Paris 7-Denis Diderot
40. Beamson G, Briggs D (eds) (1992) High resolution XPS of organic polymers. The Scienta ESCA300 database. Wiley, Chichester
41. Briggs D, Seah MP (eds) (1990) *Practical surface analysis*, 2nd edn, vol 1. Auger and X-ray photoelectron spectroscopy. Wiley, Chichester, p 209
42. Carney TJ, Tsakirooulos P, Watts JF, Castle JE (1990) *Int J Rapid Solid* 5:189